

Direct Fabrication of sub-100 nm Nanoneedles in Silver using Femtosecond Laser Direct Writing

Balaji Yendeti and Venugopal Rao Soma*

Advanced Centre for Research in High Energy Materials, University of Hyderabad, Hyderabad - 500 046, India

**E-mail: soma_venu@uohyd.ac.in*

ABSTRACT

Novel methods for production of nanomaterials are urgently needed for various applications, especially in defence. In this work, we propose a direct method to produce silver nanoneedles using the femtosecond laser direct writing (LDW) technique. Femtosecond pulses were focused by a microscope objective on to a metal sheet to produce the nanoneedles. Nanoneedles of required dimensions were fabricated with a simple replacement of microscope objective of different numerical aperture. Further, we have investigated the effect of confinement. Finally, the application of nanoneedles is demonstrated for trace level detection of picric acid using surface enhanced Raman spectroscopy and a field deployable portable Raman spectrometer.

Keywords: Laser processing; Raman; Femtosecond; Silver nanoneedles

1. INTRODUCTION

Metal nanostructures with needles/needle-like sharp structures are of major interest in drug delivery applications, probing biological cells, controlled delivery of nucleic acids to selected tissues and surface enhanced Raman spectroscopy (SERS) studies¹⁻⁴. These applications are attributed to the special mechanical characteristics like high aspect ratio, electrical and optical properties of nanoneedles. There are very few methods to produce metallic and non-metallic micro/nanoneedle structures⁵⁻⁸. Optical vortex pulses were previously used to fabricate metal nanoneedles⁸. Yang⁷, *et al.* have used confined laser spinning (CLS) method to produce gold nanoneedles. The spinning process was described as melting and evaporation of metallic thin film, explosion of vaporised film and lateral propagation to form nanoneedles. In their work, laser direct writing (LDW) onto a 30 nm thin Au film confined by ITO coated glass plate produced nanoneedles in large scale. In this letter, we followed the CLS technique with a few modifications. Specifically, to produce metal nanoneedles of different sizes in large scale, it is easier to use metal sheet rather than thin films. There are other methods, such as metal assisted chemical etching, for producing these type of nanostructures⁹. However, these methods are not suitable for etching hard metals such as silver and gold. Whereas our proposed method is suitable for creating nanostructures in soft semiconductor materials like Si and hard materials such as silver and gold simply by controlling the laser energy. Additionally, no chemicals are involved in the present method rendering this a green

technique. Herein, we present results from the LDW [using ~50 femtosecond (fs) pulses] of silver (Ag) metal sheet with different focusing conditions to produce and control the sizes of nanoneedles. Furthermore, we have investigated the consequences of confined and unconfined laser spinning. Additionally, the fabricated Ag nanoneedles were utilised as active SERS substrates for detecting an explosive molecule (picric acid) at low concentrations.

2. MATERIALS AND METHODS

An ultrafast laser system (~4 mJ, 1 kHz ~50 fs, 800 nm) was employed to perform the LDW experiments. The incident laser pulse energy was controlled by the combination of half wave plate and Brewster polariser. Two different experiments were performed as shown in Fig. 1. In the first experiment, pulses were focused by a 20X microscope objective (MO, Newport M-20X) of numerical aperture (NA) 0.40 onto silver metal sheet (Alfa Aesar, 99% pure) of dimensions 2×1.5×0.2 cm³. In the second experiment, pulses were focused with a 60X MO (Newport M-60X) and 0.85 NA onto the target and was covered on top with a microscope coverslip (130-170 μm thick). In these experiments, Ag target was placed onto a 3-dimensional (XYZ) stage and interfaced to motion controller (Newport ESP 300). The stage was programmed to move in two dimensions (X and Y) with velocity of 0.2 mm/s along X-axis and 2 mm/s along Y-axis and vice-versa in cross structure fabrication (Fig. 1(a)). Third axis was used to position the focal point of the MO onto the sample. In these experiments cross structures were fabricated on the Ag target. In first experiment, laser was focused by 20X MO directly onto the metal sheet and the Ag nanoneedles can be observed on the edges of the laser spot focused on metal sheet. In the second experiment

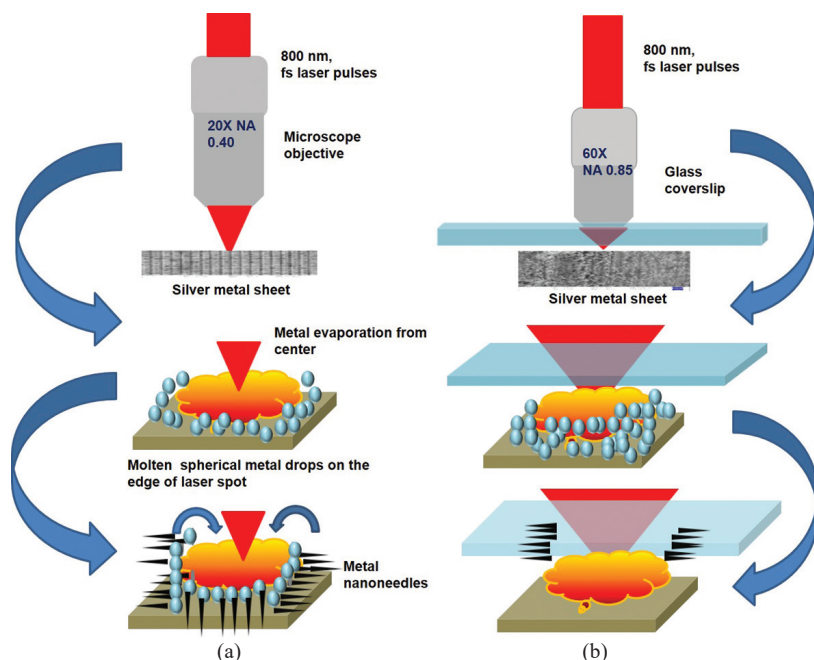


Figure 1. Schematic of fabrication of nanoneedles using LDW method with: (a) 20X objective with confinement by atmospheric pressure, and (b) confinement using glass coverslip.

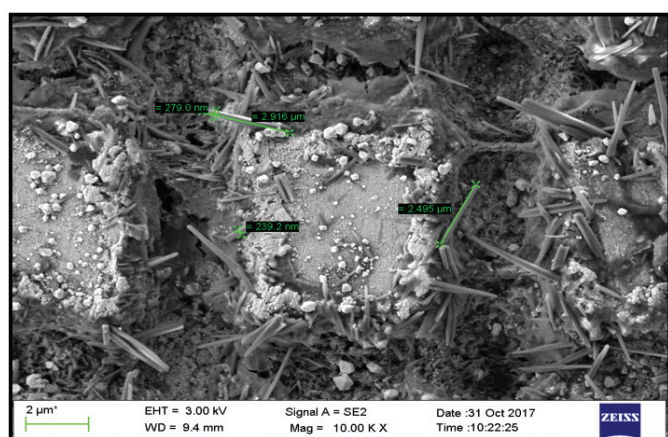
with 60X objective, laser ablated the Ag metal sheet and the nanoneedles spilled onto the coverslip placed on top of metal sheet as shown in Fig. 1(b).

The focal spot size ($2\omega_0$) with the 20X MO focusing was estimated to be $3.3 \mu\text{m}$ (measured from the line width seen in FESEM images). Since the stage traversed with a velocity of $200 \mu\text{m/s}$ and the repetition rate of the laser pulses was 1 kHz , the separation between two pulses was 200 nm . The effective number of pulses per shot was calculated using $\omega(z)/d$ and was 8 pulses/shot¹⁰. Here, $\omega(z)$ is the laser beam waist while 'd' is the separation between pulses. In case of 60X MO, focal spot size ($2\omega_0$) as measured from the line width of FESEM images was $1.6 \mu\text{m}$ (a beam waist of $0.8 \mu\text{m}$). In this case the separation between two pulses was 200 nm and the effective number of pulses was 4 per shot.

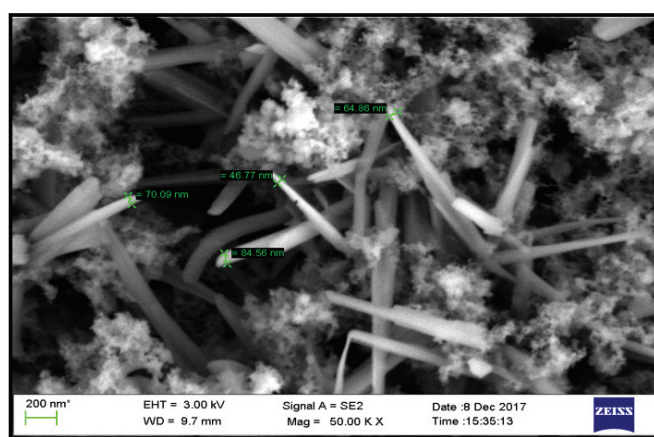
3. RESULTS AND DISCUSSIONS

The FESEM images of cross structures fabricated on silver metal sheet with 20X MO are shown in Fig. 2(a). The estimated laser fluence was 467 J/cm^2 with the input laser power being 20 mW . The measured channel width was $3.3 \mu\text{m}$ and the distance between two channels was $6.6 \mu\text{m}$. In Fig. 2(a), nanoneedles with sharp edges, high aspect ratio and smooth surface can be observed on the edges of laser spot (channel). The average width, length and sharpness of these nanoneedles were 250 nm , $2.8 \mu\text{m}$, and 20 nm , respectively. In case of LDW with 60X MO, the nanoneedles formed were confined by the microscope glass coverslip. Figure 2(b) depicts the morphology of silver nanoneedles formed on the surface of coverslip. The laser fluence with 60X microscope objective was 2000 J/cm^2 at 20 mW laser power. The packing density of nanoneedles with 60X objective on the coverslip was high when compared to the 20X objective ablation case. Figure 2(b) depicts the magnified view of nanoneedles whose average sharpness, length and width were 5 nm , $1 \mu\text{m}$, and 60 nm , respectively.

Yang⁷, *et al.* focused nanosecond (5 ns) laser pulses quickly generating high temperatures ($>$ melting point of the metal) producing molten metal drops. In that short duration metal remains as fluid with low viscosity for that period. But the spatial confinement creates high pressure shock during this laser ablation. This pressure rapidly elongates the molten metal droplets to produce nanoneedles. The sizes of nanoneedles strictly depend on the molten metal drops produced during the ablation. In case of 60X objective laser fluence was 5 times higher than 20X objectives which could have resulted in molten metal drops of very small volume¹¹. This indicates that the size of nanoneedles can be controlled by the size of molten metal drops and the size of molten metal drops in turn are controlled by spot size of focused laser beam. When a Gaussian laser beam is focused by the MO, maximum intensity at the centre of the focused laser spot is absorbed by



(a)



(b)

Figure 2. FESEM images of cross structures with : (a) 20X objective on Ag metal sheet, nanoneedles of average sharpness, width, and length of 20 nm , 250 nm and $2.8 \mu\text{m}$, respectively are on the edges of channels, (b) 60X objective on Ag metal sheet, nanoneedles of average sharpness, width, and length of 5 nm , 60 nm , and $1 \mu\text{m}$, respectively, are on the edges of channels.

the silver metal sheet surface and then vaporises. Since the laser intensity is maximum at the centre, and when it is above evaporation threshold, the metal at the centre vaporises and ionises instantly. The laser intensity is low at the edges and the metal melts and forms metal liquid droplets as shown in the schematic of Fig. 1. At the edges of laser spot, peak intensity is above melting point but below evaporation threshold. At the centre of focused laser spot, the vapour explodes violently in the confined space and continues to absorb laser energy. Continuous laser heating and condensing of vapour leads to high pressure differences inside the laser spot. This high-pressure difference expels the molten silver droplets from the laser spot edge to the exterior. These expelled low viscous metal droplets form metal nanoneedles and these re-solidified nanoneedles are obstructed by micro glass coverslip. But, in case of cross structures with 20X objective, nanoneedles can be observed despite no confinement. The possible reason is air friction acts against the direction of vaporised metal from the central portion of laser beam. Consequently, this air friction acts as a confinement mechanism for vapour. Hence, the height of confinement by the air friction is different from having a microscope coverslip. Further, the vapour explosion possibly occurs in 3 dimensions. Therefore, relatively few molten drops which are present at the edges of laser spot end up forming nanoneedles at the edges of laser spot. This results in lower packing density of the nanoneedles. The high aspect ratio and tunable nanoscale geometry of these nanoneedles make them versatile for applications like Surface enhanced Raman spectroscopy (SERS). Further detailed studies are in progress to completely understand the confinement and focusing effects in tandem.

Herein, we also present the SERS-based detection of an explosive molecule picric acid (PA) dissolved in water. The permissible exposure limit¹² of PA is 0.1 mg/m³. Trace level detection of PA in water/air environments is need of the hour. The SERS spectrum of PA recorded with nanoneedles fabricated on Ag with a 20X objective is presented in Fig. 3(a) while the reproducibility data is shown in Fig. 3(b). The localised electric field enhancement around apex of the silver nanoneedles and the surface Plasmon coupling from the nano-debris present in the periodic cross structures is responsible for stronger field enhancement of the Raman signal⁸. The sharpness of silver nanoneedles will serve as ‘hotspots’ for SERS enhancement. The major Raman peaks were observed at 820 cm⁻¹ and 1340 cm⁻¹ and are presented in Fig. 3(a) illustrates the vibrational modes of NO₂ group present in PA. These Raman modes were excited by a 785 nm (CW) laser from a field deployable, portable Raman spectrometer (B&W Tek, USA). The bulk Raman spectrum of PA (0.1 M) was recorded on Si substrate and the enhancement factor was evaluated to be 1.8×10⁶ using the standard procedure reported in literature¹³⁻¹⁴. Further, the reproducibility of these substrates was checked by recording the SERS spectra from several random locations and the relative standard deviation (RSD) values were <20%, the data of which is presented in Fig. 3(b). These nanoneedles, fabricated in the ablation process with a 20X objective, do get re-solidified and forms a strong bonding with the silver metal surface. Whereas in case of 60X objective, the nanoneedles

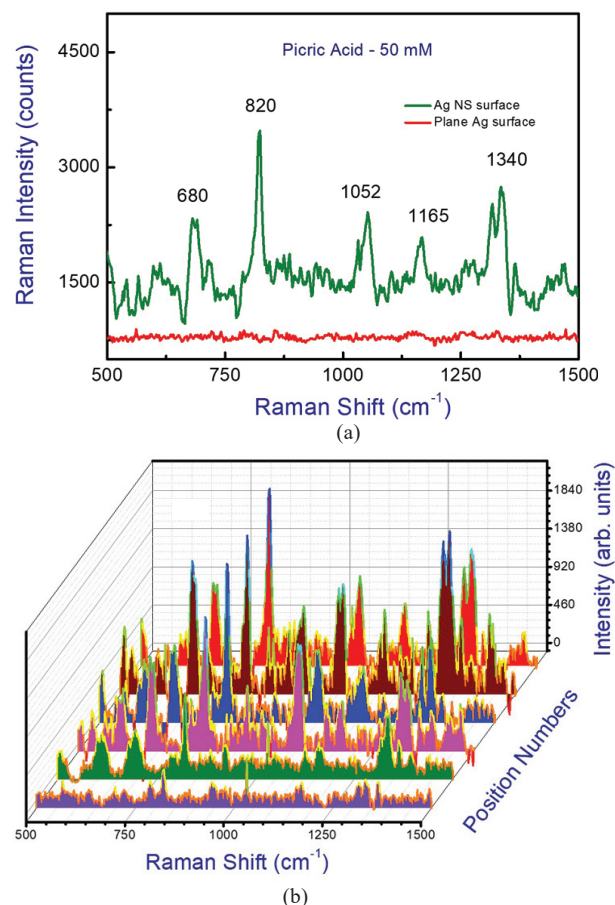


Figure 3. (a) SERS spectrum of PA recorded on plain Ag and Ag with nanoneedles (20X) (b) Reproducibility of the SERS data recorded at six different locations.

get obstructed by the coverslip and there was a poor bonding between glass coverslip and nanoneedles. SERS measurements performed on the substrate obtained with 60X objective did not result in reliable SERS measurements (though we clearly observed the enhancement). Further studies are in progress to optimise (bonding) these nanostructures and obtain consistent SERS data. This work is only a proof of concept study and our future studies will also include the investigation of different analyte molecules using these nanoneedles.

4. CONCLUSIONS

In summary, this work demonstrates the fabrication of Ag metal nanoneedles using the femtosecond LDW technique. The laser direct writing technique was investigated on a plasmonic metal (Ag) under confinement and without confinement in the formation mechanism of nanoneedles. A controlled fabrication of different sizes of metal nanoneedles is presented by simply replacing the 20X microscope objective with 60X microscope objective. Further, SERS studies on silver metal substrate containing nanoneedles demonstrated trace level detection of an important explosive molecule (picric acid) achieved with field deployable Raman spectrometer. We believe there is a huge potential for this technique and detailed studies involving different focusing conditions (in confined and no confinement geometries) are essential for realising a few practical applications of such nanostructures. The methods discussed in

this work are industry adaptable by their nature of direct, size controllable and large-scale fabrication of silver nanoneedles.

REFERENCES

1. Kathuria, H.; Kochhar, J.S. & Kang, L. Micro and nanoneedles for drug delivery and biosensing. *Ther. Deliv.*, 2018, **9**, 489-492.
doi: 10.4155/tde-2018-0012.
2. Rosi, N.L. & Mirkin, C. A. Nanostructures in Biodiagnostics. *Chem. Rev.*, 2005, **105**, 1547-1562.
doi: 10.1021/cr030067f
3. Chiappini, C.; De Rosa, E.; Martinez, J.O.; Liu, X.; Steele, J.; Stevens, M.M. & Tasciotti, E. Biodegradable silicon nanoneedles delivering nucleic acids intracellularly induce localized *in vivo* neovascularization, *Nat. Mater.*, 2015, **14**, 532-539.
doi: 10.1038/nmat4249
4. Yong, Y.; Tanemura, M.; Huang, Z.; Jiang, D.; Li, Z. Y.; Huang, Y.P.; Kawamura, G.; Yamaguchi, K. & Nogami, M. Aligned gold nanoneedle arrays for surface-enhanced Raman scattering. *Nanotechnology*, 2010, **21**, 325701.
doi: 10.1088/0957-4484/21/32/325701.
5. Nejad, H.R.; Sadeqi, A.; Kiaee, G. & Sonkusale, S. Low-cost and cleanroom-free fabrication of microneedles, *Microsystems Nanoengineering*, 2018, **4**, 17073.
doi: 10.1038/micronano.2017.73
6. Takahashi, F.; Miyamoto, K.; Hidai, H.; Yamane, K.; Morita, R. & Omatsu, T. Picosecond optical vortex pulse illumination forms a monocrystalline silicon needle. *Sci. Rep.*, 2016, **6**, 21738.
doi: 10.1038/srep21738
7. Yang, Y.; Lin, D. & Cheng, G. J. Direct writing of Au nanoneedles array on glass by confined laser spinning. *Appl. Phys. Lett.*, 2012, **101**, 091911.
doi: 10.1063/1.4746427
8. Hamazaki, J.; Morita, R.; Chujo, K.; Kobayashi, Y.; Tanda, S. & Omatsu, T. Optical-Vortex laser ablation, *Opt. Express*, 2010, **18**, 2144-2151.
doi: 10.1364/OE.18.002144
9. Zhipeng Huang, Nadine Geyer, Peter Werner, Johannes de Boor, Ulrich Gosele, Metal-assisted chemical etching of Silicon: A Review. *Advanced Materials*, 2011, **23**(2), 285-308.
doi: 10.1002/adma.201001784
10. Podagatlapalli, G. K.; Hamad, S.; Tewari, S.P.; Sreedhar, S.; Prasad M.D. & Venugopal Rao, S. Silver nano-entities through ultrafast double ablation in aqueous media for surface enhanced Raman scattering and photonics applications. *J. Appl. Phys.*, 2013, **113**, 073106.
11. Noel, S.; Hermann, J. & Itina, T. Investigation of nanoparticle generation during femtosecond laser ablation of metals. *Appl. Surf. Sci.*, 2007, **253**(15), 6310-6315.
doi: 10.1016/j.apsusc.2007.01.081
12. Hakonen, A.; Wang, F.C.; Andersson, P.O.; Wingfors, H.; Rindzevicius, T.; Schmidt, M.S.; Soma, V.R.; Xu, S. C.; Li, Y.Q.; Boisen, A. & Wu, H. A. Hand-held Femtogram detection of hazardous picric acid with hydrophobic Ag Nanopillar SERS substrates and mechanism of elastocapillarity. *ACS Sens.*, 2017, **2**(2), 198-202,
doi: 10.1021/acssensors.6b00749
13. Yin, H.J.; Chan, Y.F.; Wu, Z.L. & Xu, H. J. Si/ZnO nanocomb arrays decorated with Ag nanoparticles for highly efficient surface-enhanced Raman scattering. *Opt. Lett.*, 2014, **39**(14), 4184-4187.
doi: 10.1364/OL.39.004184
14. Bharathi, M.S.S.; Kalam, A.; Chandu, B.; Hamad, S. & Venugopal Rao, S. Instantaneous trace detection of nitro-explosives and mixtures with nanotextured silicon decorated with Ag-Au alloy nanoparticles using the SERS technique. *Analytica Chimica Acta*, 2020, **1101**, 157-168.
doi: 10.1016/j.aca.2019.12.026

ACKNOWLEDGMENT

We acknowledge DRDO, India for continuous financial support through project #ERIP/ER/1501138/M/01/319/D (R&D) dated 27.02.2017.

CONTRIBUTORS

Prof. Venugopal Rao Soma obtained his Master's and PhD from University of Hyderabad, India in 1994 and 2000, respectively. He has established Advanced Centre for High Energy Materials at University of Hyderabad. His research interests include detection of explosives using the techniques of SERS, LIBS, CARS and ultrafast laser-matter interaction. He has published 1 book, 10 book chapters, and >300 papers in journals/conference proceedings. He is Fellow of Institute of Physics, London, UK and the Telangana Academy of Sciences, Hyderabad. He is also a Senior Member of the OSA, IEEE, SPIE. In the present study he has provided the idea, supervised the research, helped in analysis of the data and writing/editing of the manuscript.

Dr Balaji Yendeti received his PhD in Physics from School of Physics, University of Hyderabad, in 2015. He did post-doctoral research at Tata Centre for Interdisciplinary Sciences, in 2016 and Advanced Centre for High Energy Materials, during 2017-19. He is currently working as project co-ordinator/Senior optical engineer in Ananth Technologies Limited (ATL), Hyderabad. His current research interests are thermal imaging and Lidar applications. In the present study he has performed all the experiments, analysed the data and participated in writing/editing of the manuscript.